Cerebral Expression of Glial Fibrillary Acidic Protein, Ubiquitin Carboxy-Terminal Hydrolase-L1, and Matrix Metalloproteinase 9 After Traumatic Brain Injury and Secondary Brain Insults in Rats

Ségolène Mrozek[1][*] (ID), Louis Delamarre[1][*], Florence Capilla[2], Talal Al-Saati[2], Olivier Fourcade[1], Jean-Michel Constantin[3] and Thomas Geeraerts[1,4]

[1]Department of Anesthesiology and Critical Care, University Hospital of Toulouse, Toulouse, France.
[2]Experimental Histopathology Department, INSERM US006-CREFRE, University Hospital of Toulouse, Toulouse, France.
[3]Department of Anesthesiology and Critical Care, University Hospital of Clermont-Ferrand, Clermont-Ferrand, France.
[4]ToNIC (Toulouse NeuroImaging Center), University Toulouse 3-Paul Sabatier, Inserm-UPS, Toulouse, France.

ABSTRACT: Glial fibrillary acidic protein (GFAP), ubiquitin carboxy-terminal hydrolase-L1 (UCH-L1), and matrix metalloproteinase 9 (MMP-9) are potential biomarkers of traumatic brain injury (TBI) but also of secondary insults to the brain. The aim of this study was to describe the cerebral distribution of GFAP, UCH-L1, and MMP-9 in a rat model of diffuse TBI associated with standardized hypoxia-hypotension (HH). Adult male Sprague-Dawley rats were allocated to Sham (n = 10), TBI (n = 10), HH (n = 10), and TBI+HH (n = 10) groups. After 4 hours, brains were rapidly removed and immunostaining of GFAP, UCH-L1, and MMP-9 was performed. Areas of interest that have been described as particularly sensitive to hypoxic insults were analyzed. For GFAP, in the neocortex, immunostaining revealed a significant decrease in strong staining for HH and TBI+HH groups compared with TBI group ($P < .0001$). For UCH-L1, the total immunostaining (6 regions of interest) reported a significant increase in strong staining ($P < .0001$) and decrease in weak staining ($P < .0001$) for the HH and TBI+HH groups compared with the Sham and TBI groups. For MMP-9, for the HH and TBI+HH groups, a significant increase in moderate ($P < .0001$) and weak staining ($P < .0001$) and a decrease in negative staining ($P < .0001$) compared with the Sham and TBI groups were observed. UCH-L1 and MMP-9 immunostainings increased after HH alone or HH combined with TBI compared with TBI alone. GFAP immunostaining decreased particularly in the neocortex after HH alone or HH combined with TBI compared with TBI alone. These three biomarkers could therefore be considered as potential biomarkers of HH insults independently of TBI.

KEYWORDS: traumatic brain injury, hypoxia, hypotension, GFAP, UCH-L1, MMP-9

Introduction

Traumatic brain injury (TBI) is a complex and heterogeneous pathological process. Similar cerebral injuries in appearance on brain imaging could have different neurologic prognoses and responses to treatment. Trying to better characterize brain injuries using biomarkers has become a research priority.[1-3]

Hypoxia and hypotension are common after TBI and are major sources of secondary brain damages, increasing mortality and worsening neurological outcome in patients with severe TBI.[4] The detection of these secondary brain insults using biomarkers could allow for better stratification and characterization of the disease.

Three biomarkers reflecting different components of the brain are promising candidates for brain injury identification:[5] *glial fibrillary acidic protein* (GFAP), *ubiquitin carboxy-terminal hydrolase-L1*

(UCH-L1), and *matrix metalloproteinase 9* (MMP-9).[6] Glial fibrillary acidic protein is a major component of the astrocytic cytoskeleton and is exclusively expressed in astrocytes. Ubiquitin carboxy-terminal hydrolase-L1 represents 1% to 5% of total soluble proteins of the brain and is specifically expressed in neurons. The temporal profiles of GFAP and UCH-L1 have been studied recently in rat model of fluid percussion TBI but to our knowledge, these biomarkers have never been studied following secondary brain insults.[7] Matrix metalloproteinases (MMPs) regulate homeostasis of the extracellular matrix (ECM) by proteolysis. They are implicated in the disruption of the blood-brain barrier (BBB) after TBI with degradation of the tight junction-related proteins and the basal lamina.[8,9]

Animal models of TBI allow to study the effects of posttraumatic insults on the brain physiology. Some brain regions seem to be more susceptible to secondary hypoxic insults such as the cortex or hippocampus.[10,11] The aim of this study was to

---

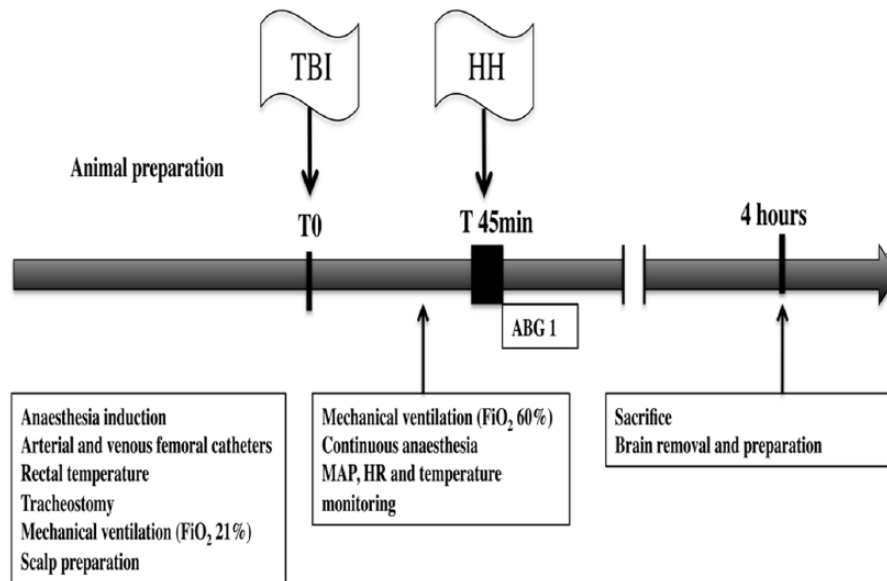* Both first authors contributed equally to this work.

Figure 1. Experimental procedure.
ABG indicates arterial blood gas; CSF, cerebrospinal fluid; FiO$_2$, inspired fraction of oxygen; HH, hypoxia-hypotension phase; HR, heart rate; MAP, mean arterial pressure; TBI, traumatic brain injury.

describe the cerebral distribution of GFAP, UCH-L1, and MMP-9 in a rat model of diffuse TBI associated with standardized hypoxia-hypotension (HH) with particular interest in regions sensitive to hypoxia. Our hypothesis was that expression of GFAP, UCH-L1, and MMP-9 could be modified by secondary hypoxic insults after TBI.

Methods and Materials

This study was undertaken in line with regulations of the Helsinki Declaration on laboratory animal care and use and the French Ministry of Agriculture. The whole methodology described below was approved by the local Ethics Committee for animal experimentation (no. B.31.555.04). The use of this standardized hypoxia-hypotension in rat model of diffuse TBI has been described in previous studies.[10,12]

Animal preparation

Adult male Sprague-Dawley rats were anesthetized in inhalation chamber with Sevoflurane (Sevorane®; Abbott, France) and then with 80 mg/kg of intraperitoneal pentobarbital sodium (Pentobarbital sodique; Ceva, France). After catheterization of the right femoral vein (Insyte-22-gauge), anesthesia was maintained by continuous intravenous infusion of pentobarbital sodium at 1 mL/h (14 mg/kg/h). Analgesia was performed with intraperitoneal xylazine (10 mg/kg, Rompun 2%®; Bayer, Germany). The right femoral artery was catheterized (Insyte-24-gauge) for continuous arterial pressure monitoring and blood withdrawal. A tracheostomy was performed (Insyte-16-gauge) and animals were mechanically ventilated with room air in prone position (Engström Carestation®; General Electric, USA; tidal volume 6-8 mL/kg, respiratory rate 60 per minute, and positive expiratory pressure [PEP] 3 cm H$_2$O).

General monitoring and experimental procedure

Rectal temperature was measured continuously with a rectal probe and animals were maintained around 37°C with heating plate (Hotplate 062® et Hotplate controller®; Bioseb, Germany). Mean arterial pressure (MAP), heart rate (HR), and temperature (T, in °C) were monitored continuously and recorded every 15 minutes during all the procedure (4 hours). These parameters were recorded every 5 minutes during the HH phase. Arterial blood gases were sampled after HH phase.

Rats were allocated randomly to the following four groups:

- Sham, in which the entire procedure was performed except head trauma and hypoxia-hypotension (HH);
- TBI, in which head trauma was performed alone;
- HH, in which HH phase was performed alone;
- TBI+HH, in which head trauma was followed by HH.

The experimental procedure is represented in Figure 1.

Adapted impact acceleration brain injury

Head trauma was realized according to the adapted model of Marmarou and colleagues[13,14] reproducing diffuse TBI with acceleration-deceleration damage without skull fracture. Our research team has used this model in previous studies.[10,12] We chose male rats because this model is validated only in male rats. A midline incision was performed on the scalp followed by periostal dissection, allowing exposing of central area in average 1.5 cm in diameter between the coronal and the lambdoid suture. A round steel disk (1-cm diameter and 3-mm thickness) was fixed by surgical cement (Palacos R-40; Schering-Plough Europe, Belgium) onto the central area of skull between bregma and lambda. Animals were then placed in prone position on a piece of

foam, under a hollow Plexiglas tube to receive a 450-g weight dropping freely from a height of 1.80 m on the steel disk. Rebound of weight was avoided by immediately moving animals after the first impact. Animals were then placed on the thermal blanket and mechanically ventilated with an oxygen-enriched mixture (inspired oxygen fraction [FiO_2]: 60%). Animals with macroscopic skull fracture, rebound impact, or dying during procedure were excluded from the final analysis. This standardized and reproducible model of severe TBI leads to diffuse axonal injury, diffuse cerebral edema, and loss of neurons.[14]

Hypoxia–hypotension phase

Hypoxia was performed by mechanical ventilation with O_2/N_2 mixture of 10%/90% (Air Liquide Santé, France) resulting in decrease in the arterial partial pressure of oxygen (PaO_2) to about 40 mmHg.[15,16] After that, hypotension was obtained with a controlled hemorrhage by bleeding via a rapid arterial withdrawal to decrease MAP to 40 mmHg. Blood was conserved in a heparinized syringe, and after 15 minutes, restored slowly (1-2 minutes) to animals. Then, animals were ventilated with oxygen-enriched mixture (FiO_2 60%). The delay between TBI and HH phase was always 45 minutes.

Sampling of brain tissue

After 4 hours of mechanical ventilation, rats were killed by exsanguination with heparinized syringe and injection of 1 mL of potassium chloride (0.1 g/mL; Fresenius Kabi, France). Brain was then rapidly removed. Three sections were performed in the frontal plane of section through origin of sylvian fissure for the most anterior section, through cerebral peduncles for posterior section, and equidistantly from the last two sections for middle section. Then, brain was sectioned on the median line to separate the right and left hemispheres. The right hemisphere was intended for immunohistochemical analysis. After fixation in 4% formaldehyde, the three parts of the right hemisphere were paraffin-embedded using a dehydration automaton (Leica TP1020®; Leica Microsystems, Germany) and then coating station (Leica EG1160®; Leica Microsystems). The three parts of the left hemispheres were coated in optimal cutting temperature (O.C.T.® Tissue-Tek®, Sakura Finetek, The Netherlands) and then immersed in a liquid nitrogen cooled isopentane for 10 to 15 seconds. Frozen pieces were then stored at −80°C.

Immunohistochemical analysis and regional distribution of biomarkers

The three paraffin sections from each animal were cut (3 μm section) on the areas of interest: neocortex, striatum, corpus callosum, and hippocampus (CA-1 region and dentate gyrus). These areas of interest have been described as particularly sensitive to hypoxic insults after TBI.[10,11] Three sections were used for immunostaining of UCH-L1 (Monoclonal Mouse

[13C4/I3C4] to PGP9.5; Abcam®, UK), GFAP (Polyclonal Rabbit Anti-Glial Fibrillary Acidic Protein, ref. Z0334; Dako®, Denmark), and MMP-9 (Monoclonal Mouse [56-2A4] to MMP-9; Abcam). After de-waxing with a series of xylene followed by 100% alcohol baths, slides were washed with distilled water. For antigen retrieval, slides were placed in a Tris/EDTA buffer at pH6 (citric acid and sodium citrate) at boiling point for 20 minutes, except for GFAP for which proteinase K proteolytic digestion was used. Slides were then incubated with the primary antibodies at a dilution of 1/500 for 30 minutes for the anti-GFAP antibodies, 12 hours for the anti-UCH-L1 antibodies, and at a concentration of 2 μg/mL for 1 hour for the anti-MMP-9 antibodies. After rinsing, slides were incubated with peroxidase-labeled secondary antibodies for UCH-L1 (ImmPRESS® Peroxidase Anti-Rabbit Ig Vector; Vector Labs, UK) and for GFAP and MMP-9 (ImmPRESS Peroxidase Anti-Mouse Ig Vector; Vector Labs). After 30 minutes of incubation by 3,3′-diaminobenzidine (DAB; ImmPACT DAB; Vector Labs), counterstain with hematoxylin was performed after immunostaining. Slides were dehydrated by successive baths in alcohol (100%) followed by xylene and then mounted (EUKITT® adhesive; Sigma–Aldrich®, USA). Slides were scanned (Pannoramic 250 Scanner®; 3DHISTECH Ltd, Hungary) and analyzed to measure the marking density in regions of interest. On each slide, regions of interest were defined with an atlas of the Sprague-Dawley rat brain in stereotactic coordinates.[17] The virtual slides were then analyzed by densitometry (Quant Center®; 3DHISTECH Ltd). The pixels were classified with an intensity score: negative, weak, moderate, or strong positive pixels for marking density.[18-20] The ratio of strong, moderate, weak positive, and negative pixels to total pixels was analyzed in total for each brain and then for each region of interest to evaluate the regional distribution of the immunostaining. So, four categories of staining intensity were described with percentage of strong, moderate, weak positive, and negative (no staining) pixels: strong staining, moderate staining, weak staining, and negative staining.

Antibody characterization

Immunohistochemical staining was performed on paraffin-embedded tissue sections, using polyclonal and monoclonal primary antibodies summarized in Table 1. Immunostaining of paraffin sections was preceded by different antigen unmasking methods. After incubation with primary antibodies, sections were incubated with peroxidase-labeled secondary antibodies (ImmPRESS™ Peroxidase Anti-Mouse or Anti-Rabbit Ig Vector; Vector Labs) followed by the DAB chromogen solution and were then counterstained with hematoxylin. Negative controls were incubated in buffered solution without primary antibody.

Statistical analysis

General and immunostaining data were compared between groups using Kruskal-Wallis test. If necessary, post hoc analysis

Table 1. Antibodies used for histological analysis.

ANTIGEN	CLONE (NUMBER)	SUPPLIER	DILUTION	INCUBATION TIME	ANTIGEN RETRIEVAL
GFAP	Rabbit polyclonal (Z0344)	Dako	1:500	1 hour	Proteinase K proteolytic digestion
UCH-L1/PGP9.5	13C4/13C4 mouse mAb (Ab8189)	Abcam	1:500	O/N	HIER/citrate pH6/MO
MMP-9	56-2A4 mouse mAb (ab58803)	Abcam	1:500	1 hour	HIER/citrate pH6/MO

Abbreviations: Ab, antibody; HIER, heat-induced epitope retrieval; mAb, monoclonal antibody; MO, boiling in microwave oven twice 10 minutes each; O/N, overnight at 4°C.

Table 2. Causes for exclusion in each group.

	SHAM GROUP	TBI GROUP	HH GROUP	TBI+HH GROUP
Early death				
Refractory shock	1	1	2	1
CPA per HH	–	–	1	0
Embolism	0	3	0	0
Skull fracture	–	0	–	0
Total	1/11 (9%)	4/14 (28.6%)	3/13 (23.1%)	1/11 (9%)

Abbreviations: CPA, cardiopulmonary arrest; HH, hypoxia-hypotension; TBI, traumatic brain injury.

was performed using the Fisher probabilistic least significant difference test. Hemodynamic consequences of TBI and HH were compared between different groups using a two-way analysis of variance (ANOVA). Differences at the level of $P < .05$ were considered statistically significant. Data are expressed as mean ± standard error of the mean (SEM). StatView 5.0® software (SAS institute Inc, USA) was used for statistical analysis.

Results

In total, 49 rats were studied but 9 (18.4%) were excluded for final analysis because of early death following refractory shock, cardiopulmonary arrest during the HH phase, or accidental embolism (Table 2). No skull fracture was reported for TBI or TBI+HH group. Thereby, 40 rats were retained, allocated randomly to each of the four groups: Sham (n = 10), TBI (n = 10), HH (n = 10), and TBI+HH (n = 10).

Physiologic characteristics and hemodynamic parameters

Animals' weights were similar between the 4 groups: Sham (498 ± 23 g), HH (470 ± 4 g), TBI (473 ± 5 g), and TBI+HH (508 ± 27 g) ($P = .69$). Rectal temperatures were comparable between the 4 groups overtime ($P = .07$). At T0, the temperature was 36.2°C ± 0.2°C, 36.2°C ± 0.2°C, 36.0°C ± 0.2°C, and 35.7°C ± 0.2°C in Sham, HH, TBI, and TBI+HH groups, respectively. After 4 hours, the temperature was 37.5°C ± 0.2°C, 37.3°C ± 0.1°C, 37.5°C ± 0.3°C, and 37.5°C ± 0.1°C in Sham, HH, TBI and TBI+HH groups, respectively. The volume of

blood depletion during the HH phase was not significantly different between HH and TBI+HH groups (5.2 ± 0.3 mL vs 5.6 ± 0.6 mL, $P = .54$).

For hemodynamic parameters, at T0, MAP was not significantly different between the 4 groups ($P = .22$; Figure 2). At 60 minutes, corresponding to the end of the HH phase just before blood reinjection in groups subjected to HH, MAP was not different between HH and TBI+HH groups (45 ± 2 mmHg vs 45 ± 2 mmHg, $P = .79$). After the HH phase, MAP was comparable for the 4 groups ($P = .75$). At the end of the procedure (4 hours), MAP for Sham, TBI, HH, and TBI+HH groups was 98 ± 5 mmHg, 102 ± 3 mmHg, 97 ± 6 mmHg, and 96 ± 3 mmHg, respectively. For blood gases, at the end of the HH phase, PaO_2 in HH and TBI+HH groups was not significantly different (51 ± 4.5 mmHg vs 44.9 ± 6.5 mmHg, $P = .48$).

Glial fibrillary acidic protein immunostaining

Glial fibrillary acidic protein immunostaining was present in all groups and no negative staining was reported. Moderate immunostaining was not different between the 4 groups. Analysis of all regions of interest revealed a significant decrease in percentage of strong staining and increase in percentage of weak staining for the TBI, HH, and TBI+HH groups compared with Sham group (Table 3; Figure 3). There was no difference between TBI and TBI+HH groups for GFAP strong and weak staining.

Table 3 represents the percentages of strong and weak staining according to the 6 different regions of interest. In the neocortex,
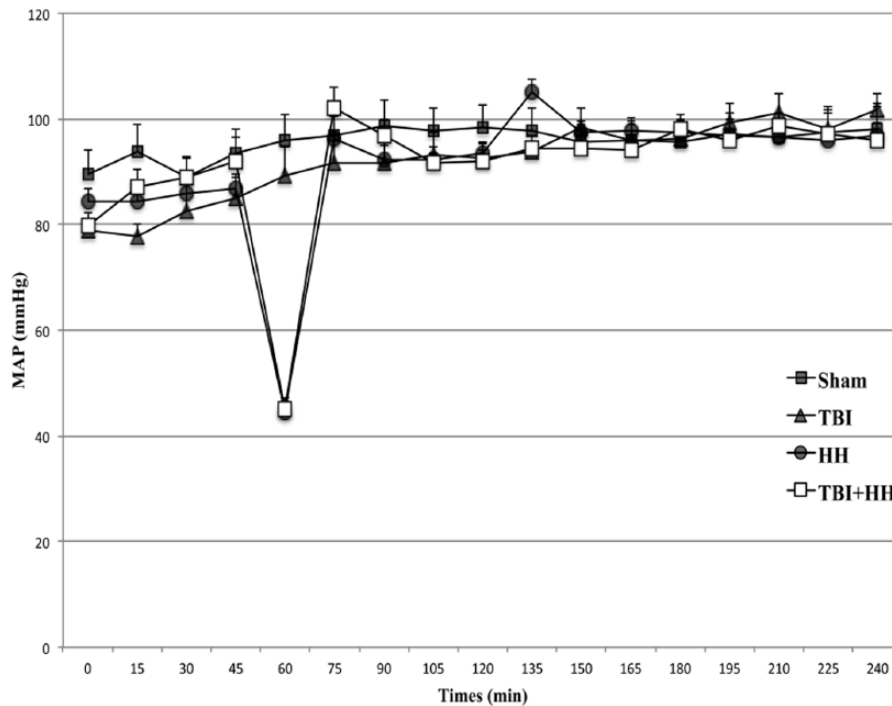
Figure 2. Mean arterial pressure during procedure for each group.
Values are represented as mean±SEM. HH indicates hypoxia-hypotension; SEM, standard error of the mean; TBI, traumatic brain injury.

Table 3. Ratio of strong positive pixels (strong staining) on total pixels and weak positive pixels (weak staining) on total pixels for GFAP for the 6 different regions of interest and for all regions.

	GFAP							
	SHAM		TBI		HH		TBI+HH	
	STRONG STAINING (%)	WEAK STAINING (%)	STRONG STAINING (%)	WEAK STAINING (%)	STRONG STAINING (%)	WEAK STAINING (%)	STRONG STAINING (%)	WEAK STAINING (%)
Neocortex	36.9±2.1	16.4±3.1	24.3±1.1*	28.7±2.3	17±0.7*§	32.9±1.6*	17.1±1*§	32.4±2.1*
Striatum	28.4±1.8	19.7±3.1	18.5±2.3*	35.1±3.5*	17.7±1.2*	34.5±2.2*	20.4±1.8*	31.4±3*
Thalamus	27.7±1.3	19.9±3.2	20.1±1.5	25.4±3.1	20.9±1.6	27.1±2.3	20.8±1.8	25.3±2.6
Dentate gyrus	38.7±3.4	10.6±2.4	29±2	18.1±2.4	30.8±2.1	18.1±2.3	29.4±3.6	21.2±3.6
CA-1 region	35.7±3.1	12.3±2.3	29.7±2.3	16.4±2.4	28.8±2.1	18.4±2.5	29.7±3.1	17.9±3.3
Corpus callosum	37.2±4.9	11±3	33±4.7	17.6±3.6	27.7±1.6	17.1±2.1	28.8±1.6	14.9±1.9
All regions	34±1.3	15.1±1.3	25.5±1.2*	23.8±1.5*	21.8±0.7*§	27.1±1.1*	22.5±0.9*	26±1.3*

Abbreviations: GFAP, glial fibrillary acidic protein; HH, hypoxia-hypotension; SEM, standard error of the mean; TBI, traumatic brain injury.
Ratios are expressed in percentage of total pixels. Data are expressed in mean±SEM.
*$P<.05$ vs Sham group. §$P<.05$ vs TBI group.

immunostaining revealed a significant decrease in percentage of strong staining for TBI, HH, and TBI+HH groups compared with Sham group. We reported a significant decrease in percentage of strong staining for HH and TBI+HH groups compared with TBI group. In parallel, a significant increase in weak staining was found for HH and TBI+HH groups compared with Sham group. In the striatum, a significant decrease in percentage of strong staining and a significant increase in percentage of weak staining were found for the TBI, HH, and TBI+HH groups

compared with Sham group. A similar trend was observed in the thalamus, dentate gyrus, CA-1 region, and corpus callosum without reaching statistical significance.

Ubiquitin carboxy-terminal hydrolase–L1 immunostaining

As for GFAP, UCH-L1 immunostaining was present in all groups and no negative staining was reported. Moderate
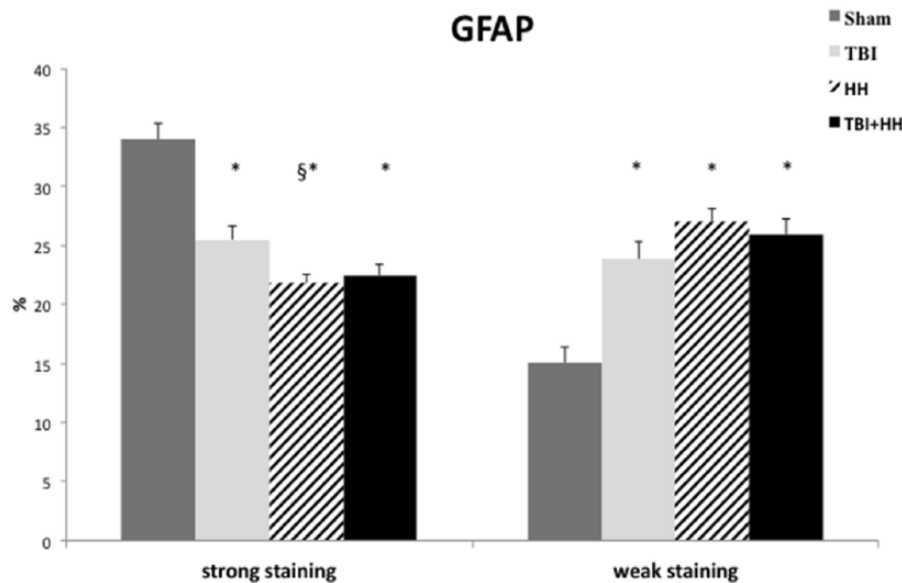
Figure 3. Ratio of strong positive pixels (strong staining) on total pixels and weak positive pixels (weak staining) on total pixels for GFAP. Data are expressed in mean ± SEM. We can note a significant decrease in percentage of strong staining and increase in percentage of weak staining for the TBI, HH, and TBI+HH groups compared with Sham group. GFAP indicates glial fibrillary acidic protein; HH, hypoxia-hypotension; SEM, standard error of the mean; TBI, traumatic brain injury.

immunostaining was similar for the 4 groups. Analysis of all regions of interest revealed a significant increase in percentage of strong staining and decrease in percentage of weak staining for the HH and TBI+HH groups compared with the Sham and TBI groups (Table 4; Figure 4).

Table 4 represents the percentages of strong and weak staining according to the 6 different regions of interest. In the neocortex, a significant increase in percentage of strong staining and a significant decrease in percentage of weak staining were observed for the TBI, HH, and TBI+HH groups compared with Sham group. In the striatum, a significant increase in percentage of strong staining and decrease in percentage of weak staining for the HH and TBI+HH groups were found compared with the Sham and TBI groups. In the dentate gyrus, CA-1 region, and corpus callosum, an increase in percentage of strong staining and a decrease in percentage of weak staining were observed for the HH group compared with the Sham and TBI groups. For the TBI+HH group, an increase in percentage of strong staining in the dentate gyrus compared with the Sham group was observed and in the corpus callosum compared with the Sham and TBI groups. In the dentate gyrus, the percentage of weak staining was decreased for the TBI+HH groups compared with the Sham and TBI groups. In the CA-1 region and the corpus callosum, we reported a decrease in the percentage of weak staining for the TBI+HH group compared with the Sham group.

Matrix metalloproteinase 9 immunostaining

Strong immunostaining was not observed for MMP-9 in all groups. Moderate, weak positive staining and negative staining were reported. For the HH and TBI+HH groups, a significant increase in percentage of moderate and weak staining and decrease in percentage of negative staining were found compared with the Sham and TBI groups (Table 5; Figure 5).

Table 5 represents the percentages of moderate, weak, and negative staining according to the 6 different regions of interest. For all regions of interest, the HH and TBI+HH groups presented a significant increase in percentage of moderate staining and decrease in percentage of negative staining compared with the Sham and TBI groups. Figures 6 and 7 represent, respectively, the cortex and hippocampus (dentate gyrus and CA-1 region) staining for the 3 biomarkers in the 4 groups. Figure 8 represents the immunohistochemical staining patterns of GFAP, UCH-L1, and MMP-9 proteins in each group with magnification at ×40.

Discussion

We described here global and regional immunostaining of GFAP, UCH-L1, and MMP-9 after standardized secondary hypoxic insult in a rat model of diffuse TBI. Ubiquitin carboxy-terminal hydrolase-L1 and MMP-9 immunostainings increased after HH alone or HH combined with TBI compared with TBI alone globally and in different regions particularly sensitive to hypoxic insults. Glial fibrillary acidic protein immunostaining decreased, particularly in the neocortex, after HH alone or HH combined with TBI compared with TBI alone.

Glial fibrillary acidic protein, UCH-L1, and MMP-9 were chosen due to their expression in three different components of the brain: astrocytes, neurons, and extracellular matrix. Glial fibrillary acidic protein is a brain-specific protein located in the cytoskeleton of astrocytes. Its expression is specific to glial cells, forming a filament network that provides support to the cell. Ubiquitin carboxy-terminal hydrolase-L1 represents 1% to 5%

Table 4. Ratio of strong positive pixels (strong staining) on total pixels and weak positive pixels (weak staining) on total pixels for UCH-L1 for the 6 different regions of interest and for all regions.

	UCH-L1							
	SHAM		TBI		HH		TBI+HH	
	STRONG STAINING (%)	WEAK STAINING (%)	STRONG STAINING (%)	WEAK STAINING (%)	STRONG STAINING (%)	WEAK STAINING (%)	STRONG STAINING (%)	WEAK STAINING (%)
Neocortex	6.4±1.3	17.7±4.1	11.1±2.1*	9.6±3*	13.1±1*	5.2±0.7*	13.2±1.2*	6.6±1*
Striatum	5.5±1.4	23.4±8.9	5±1.3	18.7±6.1	16.6±2.4*§	4.7±1.6*§	14.9±2.3*§	7.1±2.1*§
Thalamus	9.3±5.9	21.7±7	16.1±5.8	12.9±5.9	24.4±2.3	4.1±0.8	19.6±2.7	6.4±1.2
Dentate gyrus	5±1.5	20.3±6.5	6.4±2.3	19.3±4.7	14.7±2.1*§	4.5±0.8*§	12.6±2.1*	6.6±2.5*§
CA-1 region	7.5±1.8	18±4.7	7.3±1.9	12.9±3.1	18.4±1.8*§	3.1±0.5*§	13.1±2.7	5.5±1.7*
Corpus callosum	8.4±2.6	14.6±3.5	6.9±1.3	13.5±5.7	17.1±1.8*§	5.1±1.1*§	18.2±4.2*§	5.8±1.3*
All regions	7±0.9	18.2±2.2	9.5±1.2	13.1±1.8*	15.7±0.7*§	4.7±0.4*§	14.3±0.9*§	6.4±0.6*§

Abbreviations: HH, hypoxia-hypotension; SEM, standard error of the mean; TBI, traumatic brain injury; UCH-L1, ubiquitin carboxy-terminal hydrolase-L1.
Ratios are expressed in percentage of total pixels. Data are expressed in mean±SEM.
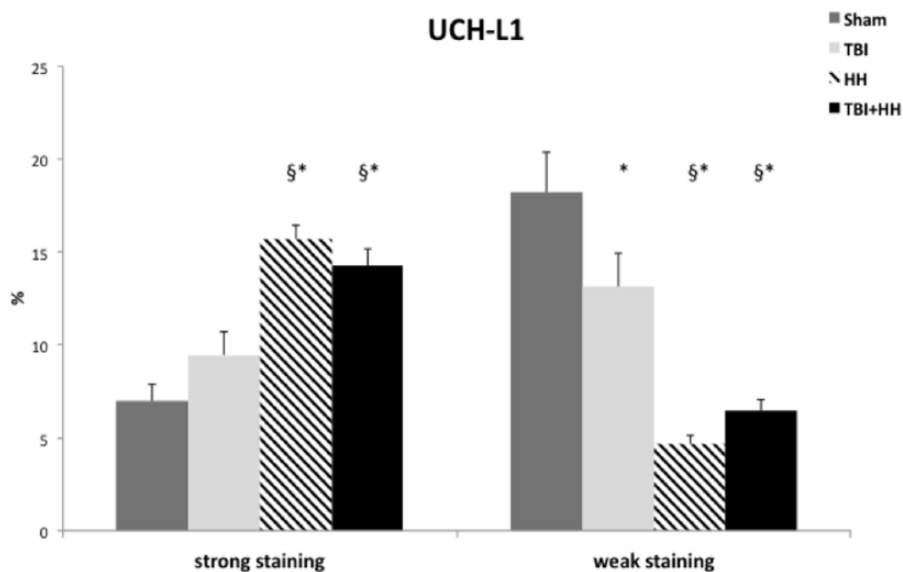*P<.05 vs Sham group. §P<.05 vs TBI group.

Figure 4. Ratio of strong positive pixels (strong staining) on total pixels and weak positive pixels (weak staining) on total pixels for UCH-L1. Data are expressed in mean±SEM. We can note a significant increase in percentage of strong staining and decrease in percentage of weak staining for the HH and TBI+HH groups compared with the Sham and TBI groups. HH indicates hypoxia-hypotension; SEM, standard error of the mean; TBI, traumatic brain injury; UCH-L1, ubiquitin carboxy-terminal hydrolase-L1.

of total soluble proteins of the brain and is mainly expressed in neurons.[21] It is implicated in the addition and depletion of ubiquitin-dependant proteins and plays a major role in the suppression of abnormal, excessive, or oxidized proteins in physiological or pathological conditions. Matrix metalloproteinase 9 is an inductive enzyme of the zinc-dependent endopeptidase family. It regulates homeostasis of the extracellular matrix by proteolysis.[22] Matrix metalloproteinase 9 is very weakly present in healthy brain tissue, but its expression increases rapidly after brain injuries such as ischemic stroke[23]

and TBI.[9] In humans, UCH-L1 and GFAP concentrations in the plasma have been correlated with the initial severity of TBI (Glasgow Coma Score), brain injuries on imaging at admission, neurological outcome, and mortality.[24,25] Matrix metalloproteinase 9 has been less studied in TBI. However, concentrations in the cerebrospinal fluid (CSF) and plasma are elevated after moderate and severe TBI and MMP-9 seems to be correlated with neurological outcome and mortality.[26-29]

In experimental model of moderate parasagittal fluid percussion TBI in rats, the time course of GFAP changes in the

Table 5. Ratio of moderate positive pixels (moderate staining) on total pixels, weak positive pixels (weak staining) on total pixels, and negative pixels (negative staining) on total pixels for MMP-9 for the 6 different regions of interest and for all regions.

	MMP-9											
	SHAM			TBI			HH			TBI+HH		
	MODERATE STAINING (%)	WEAK STAINING (%)	NEGATIVE STAINING (%)	MODERATE STAINING (%)	WEAK STAINING (%)	NEGATIVE STAINING (%)	MODERATE STAINING (%)	WEAK STAINING (%)	NEGATIVE STAINING (%)	MODERATE STAINING (%)	WEAK STAINING (%)	NEGATIVE STAINING (%)
Neocortex	2.2±0.4	57.1±4.8	40.4±5	2.3±0.1	57.2±4.2	39.8±4.2	15.2±2.4*§	77.2±2.1*§	7.1±0.7*§	16.2±2.6*§	74.8±2.4*§	7.8±0.8*§
Striatum	2.4±0.3	68.4±3.7	28.9±3.5	1.7±0.2	53.2±8.7	44.8±8.8*	18.9±4.1*§	72.5±3.5	8.1±1.8*§	18.2±4.5*§	72.2±3.7	9±2.4*§
Thalamus	3.6±0.6	62.3±5.7	33.5±5.7	3.1±0.2	68.3±2.9	28±3	27.4±6.4*§	66.6±5.8	5.2±1.1*§	25.8±6.3*§	65.6±5.8	7.8±1.7*§
Dentate gyrus	3.1±0.6	65.9±6.7	30.5±7	2.1±0.1	64.9±4.1	32.6±4.2	27.9±7.1*§	65.4±6.5	5.8±1*§	32.7±7.2*§	60.3±6.4	5.8±1*§
CA-1 region	2.1±0.3	68.3±6.7	29.4±6.9	1.6±0.1	65±4.7	32.9±4.7	26.7±7.5*§	67.1±6.9	5.7±1.1*§	32.3±8.8*§	61±7.9	6±1.4*§
Corpus callosum	4±0.9	40.8±6.1	54.6±6.1	2±0.4	40.2±8.4	57.5±8.5	22.4±5.7*§	67.7±5.1*§	9.4±1.3*§	23.2±5.5*§	62.8±4.4*§	13.4±3.1*§
All regions	2.8±0.2	58.7±2.7	38.1±2.7	2.2±0.1	58.5±2.4	38.8±2.5	20.8±1.9*§	71.7±1.7*§	7±0.5*§	22.3±2.1*§	68.5±1.8*§	8.2±0.7*§

Abbreviations: HH, hypoxia-hypotension; MMP-9, matrix metalloproteinase 9; SEM, standard error of the mean; TBI, traumatic brain injury.
Ratios are expressed in percentage of total pixels. Data are expressed in mean ± SEM.
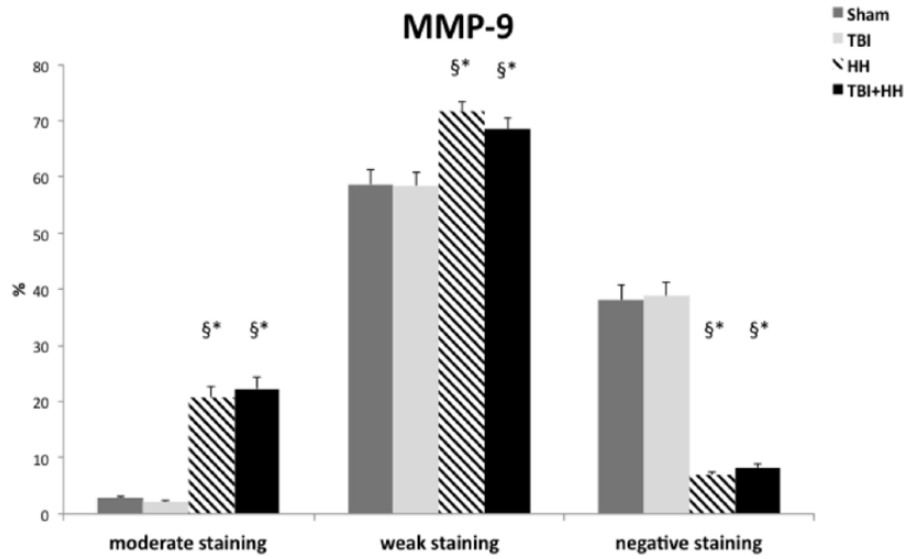*$P < .05$ vs Sham group. §$P < .05$ vs TBI group.

Figure 5. Ratio of moderate positive pixels (moderate staining) on total pixels, weak positive pixels (weak staining) on total pixels, and negative pixels (negative staining) on total pixels for MMP-9.

Data are expressed in mean±SEM. For the HH and TBI+HH groups, a significant increase in percentage of moderate and weak staining and decrease in percentage of negative staining were found compared with the Sham and TBI groups. HH indicates hypoxia-hypotension; MMP-9, matrix metalloproteinase 9; SEM, standard error of the mean; TBI, traumatic brain injury. *P < .05 vs Sham group. §P < .05 vs TBI group.
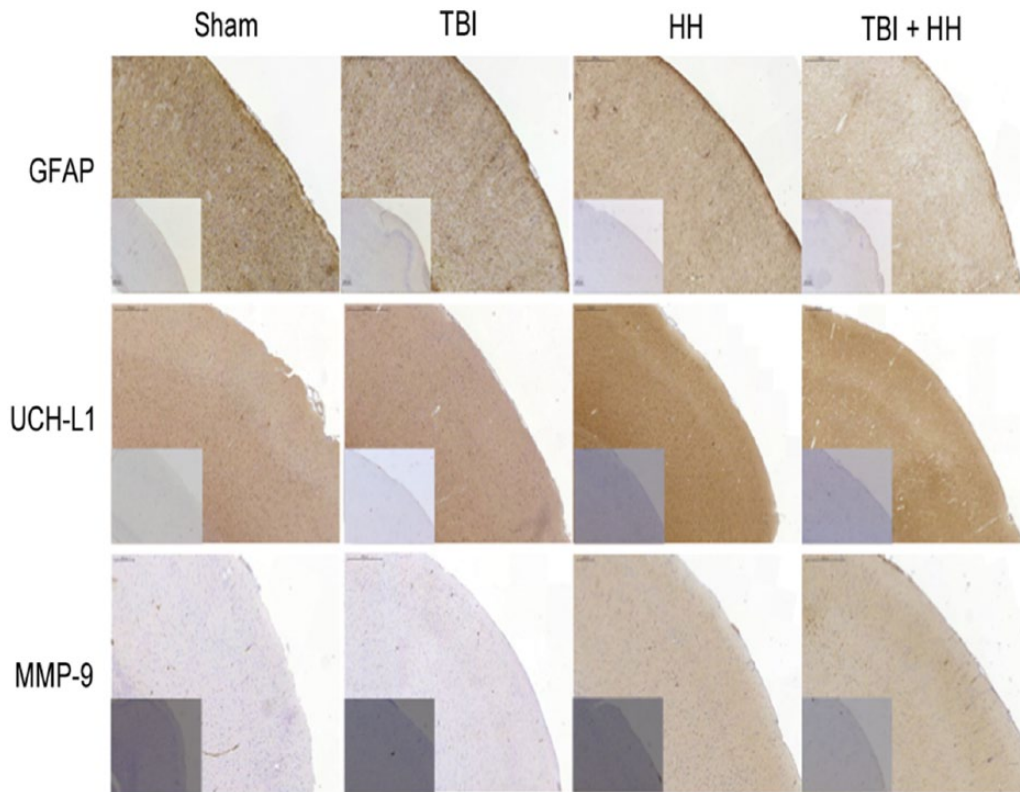

Figure 6. Cortex staining for GFAP, UCH-L1, and MMP-9 in each group.

Boxes at the bottom left represent isotype-specific control images without primary antibody for each groups and each biomarkers. We can note less intensive GFAP immunostaining in the neocortex after HH and TBI+HH compared with TBI alone. For UCH-L1, immunostaining is more pronounced for TBI, HH, and TBI+HH groups compared with Sham group. For MMP-9, there is more intensive immunostaining for HH and TBI+HH groups compared with Sham and TBI alone groups. GFAP indicates glial fibrillary acidic protein; HH, hypoxia/hypotension group; MMP-9, matrix metalloproteinase 9; Sham, Sham group; TBI, traumatic brain injury group; TBI+HH, traumatic brain injury and hypoxia/hypotension group; UCH-L1, ubiquitin carboxy-terminal hydrolase-L1.
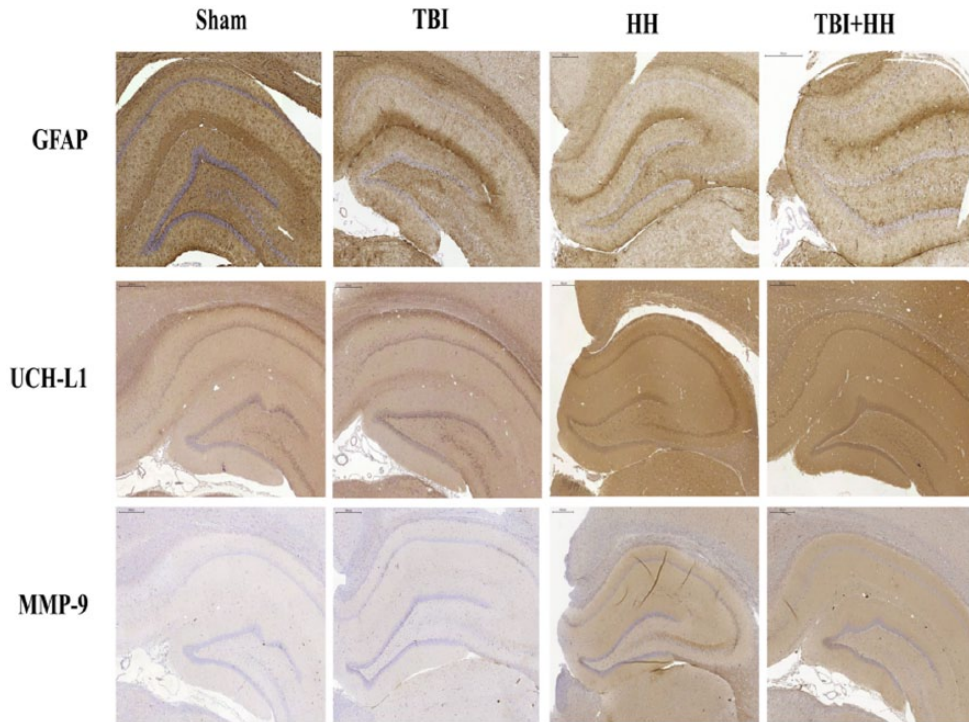
Figure 7. Hippocampus staining for GFAP, UCH-L1, and MMP-9 in each group.
We can note trend to less intensive GFAP immunostaining in the hippocampus (dentate gyrus + CA-1 region) after HH and TBI+HH compared with TBI alone. For UCH-L1 and MMP-9, immunostaining is more pronounced for HH and TBI+HH groups compared with Sham and TBI alone groups. GFAP indicates glial fibrillary acidic protein; HH, hypoxia/hypotension group; MMP-9, matrix metalloproteinase 9; Sham, Sham group; TBI, traumatic brain injury group; TBI+HH, traumatic brain injury and hypoxia/hypotension group; UCH-L1, ubiquitin carboxy-terminal hydrolase-L1.
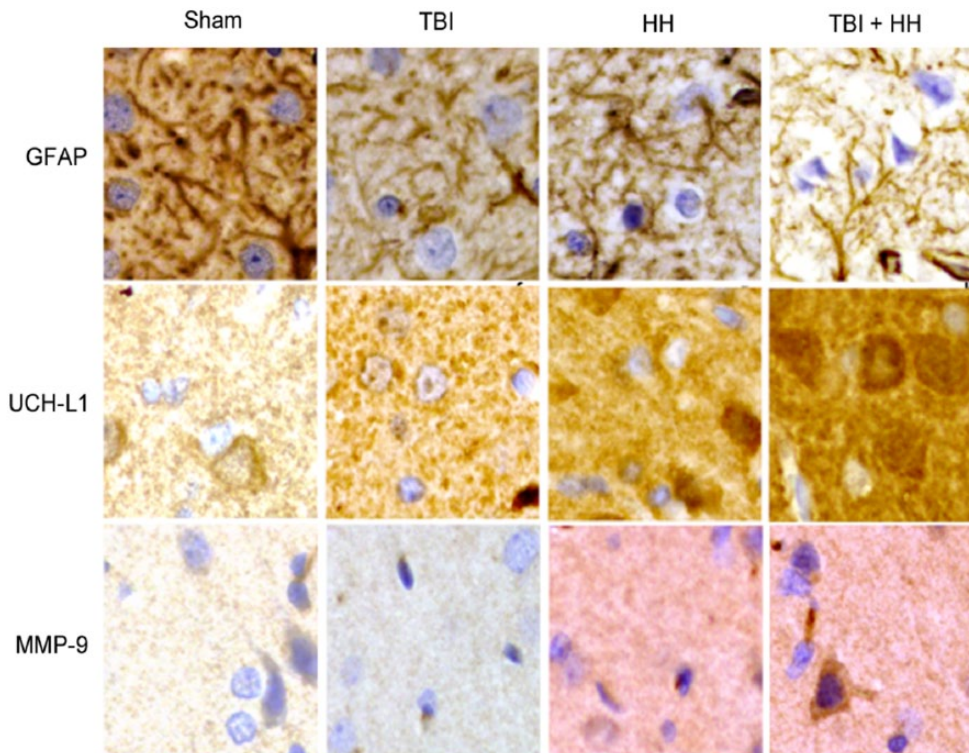

Figure 8. Immunohistochemical staining patterns of GFAP, UCH-L1, and MMP-9 proteins in each group: Sham, TBI, HH, and TBI+HH in the neocortex.
All magnifications are at ×40. GFAP proteins form filament network in cytoskeleton and staining is less intensive in TBI, HH, and TBI+HH groups compared with Sham group. UCH-L1 proteins have diffuse and granulated staining with more intensive staining in the TBI, HH, and TBI+HH groups compared with sham group. For MMP-9, stainings are almost inexistant for Sham and TBI groups and are marked and diffuse for HH and TBI+HH groups. GFAP indicates glial fibrillary acidic protein; HH, hypoxia/hypotension group; MMP-9, matrix metalloproteinase 9; Sham, Sham group; TBI, traumatic brain injury group; TBI+HH, traumatic brain injury and hypoxia/hypotension group; UCH-L1, ubiquitin carboxy-terminal hydrolase-L1.

plasma and CSF has been described. Huang et al[7] reported a significant increase in plasmatic GFAP concentrations at 3 and 6 hours and of CSF GFAP concentrations at 24 hours after TBI. Histologic analysis at 24 hours after TBI reported a decrease in GFAP immunostaining in areas where neuron loss was observed (cortex and hippocampus). Huang et al argued that the areas of reduced GFAP immunostaining presented a loss of morphologically intact astrocytes and possible injured astrocytes (in the same areas of neuronal degeneration). Another study with moderate fluid percussion TBI reported a decrease in GFAP immunostaining as soon as 30 minutes after TBI in areas (parietal cortex and hippocampus) where neuronal loss was found in the following days.[30] Therefore, increases in plasmatic and CSF GFAP concentrations increase after TBI are likely due to astrocyte damages and not to reactive astrocytes. Previous studies concluded that reactive astrocytes are observed later in experimental TBI.[30,31] Our study confirms that GFAP changes occur early after TBI (4 hours), and we reported for the first time that decreases in GFAP staining were worsened by hypoxia-hypotension after TBI in the neocortex compared with TBI alone. Secondary insults such as hypoxia-hypotension could worsen astrocyte disintegration in regions particularly sensitive to hypoxic insults. The concept of post-traumatic brain vulnerability that has been developed in recent years suggests that after TBI, regions of interest in the brain may be more susceptible to post-traumatic hypoxic insults.[11,32] Our team reported previously a particular cortical vulnerability to hypoxia-hypotension after TBI in rat model.[10] Secondary brain damages could therefore be characterized in part by the worsening of astrocytes injuries in the neocortex.

Ubiquitin carboxy-terminal hydrolase-L1 has a high affinity for ubiquitin and plays a major role in the ubiquitin proteasome system (UPS) by acting as deubiquitinating enzymes (DUBs).[33] Ubiquitin carboxy-terminal hydrolase-L1 allows for the generation of free monomeric ubiquitin from ubiquitin precursors and has ubiquitin ligase activity. In addition, UCH-L1 binds to ubiquitin to inhibit its degradation.[34] The regulation of the UPS and DUBs involves a very complex pathway that is not well understood, particularly in TBI.[35] A recent meta-analysis suggested a potential utility of UCH-L1 for the diagnosis and prognosis of patients with TBI.[24] In our study, global strong staining significantly increased in the TBI+HH group compared with the TBI alone group, and global weak staining decreased. So, there was more intensive UCH-L1 immunostaining in the TBI+HH group than in the TBI-alone group. These changes were reported in the striatum, and a similar trend (without reaching statistical significance) was described in other regions of interest. Huang et al reported a significant increase in plasmatic UCH-L1 concentrations at 3 hours TBI in a rat model of moderate parasagittal fluid percussion TBI, with normalization at 6 hours. Cerebrospinal fluid UHC-L1 concentrations are increased at 24 hours compared with a Sham group, whereas plasmatic concentrations are normalized likely from restoration of the integrity of the BBB. Histologic analysis

at 24 hours revealed typical neuronal degeneration in the parietal cortex and hippocampus, explaining UCH-L1 CSF and plasmatic increase.[7] In our study, post-traumatic hypoxic insults increase UCH-L1 staining. Brain ischemia or hypoxia likely induces excessive accumulation of ubiquitinated proteins that will be degraded by the proteasome.[36] Overproduction of misfolded proteins after ischemia or hypoxia may be reflected by an increase in the conjugation of targeted proteins with ubiquitin.[37] In our study, UCH-L1 staining was similar in the TBI+HH and HH groups, so UCH-L1 changes seem to reflect a hypoxic insult alone and are not specific to post-traumatic hypoxic secondary insults. We can hypothesize that hypoxia-hypotension leads to the production of damaged proteins and the excessive accumulation of UCH-L1 through UPS. Majetschak et al[35] reported a more than 4-fold increase in CSF ubiquitin levels in patients with TBI.

Matrix metalloproteinases regulate homeostasis of the extracellular matrix by proteolysis of its components. Matrix metalloproteinases are present at basal levels in the central nervous system (CNS), specifically in neurons, astrocytes, endothelial cells, and myelinated fibers. However, their basal level of activity is relatively low.[38] An up-regulation of MMP activity, particularly MMP-9, an inducible MMP, has been reported after acute cerebral injuries in neuroinflammatory conditions such as spinal cord injury, cerebral ischemia, or TBI.[9,39] Hadass et al[40] reported an increase in proMMP-9 and activated MMP-9 in the injured cortex within 24 hours in a controlled cortical impact model of TBI, followed by a rapid decrease in activated MMP-9 after one day. Matrix metalloproteinases are implicated in the disruption of the BBB after TBI due to the degradation of tight junction-related proteins and the basal lamina.[8,9] Shigemoni et al described an increase in MMP-9 activity as early as 3 hours, as well as an association with opening of the BBB and brain edema formation in a controlled cortical impact model of TBI. In the present study, strong staining of MMP-9 was not observed and negative staining was reported likely because MMP-9 is an inducible enzyme and not present at basal level. We reported here significant increases in percentage of moderate and weak staining and a decrease in percentage of negative staining in the cortex and corpus callosum for the TBI+HH and HH groups compared with the TBI and Sham groups. So, there was more intensive MMP-9 immunostaining in the TBI+HH and HH groups compared with the others. The same findings were observed for moderate and negative staining in other brain regions of interest. Secondary hypoxic insults after TBI led to an increase in MMP-9 immunostaining in all regions of interest compared with TBI alone, likely reflecting post-traumatic brain vulnerability. Matrix metalloproteinase 9 could be up-regulated after hypoxic insults and participate to secondary brain damages with edema formation. Regulation of MMP-9 occurs at multiple levels particularly with an activator protein-1 (AP-1) site in the gene promoter region. Moreover, MMP-9 has a nuclear factor-κB (NF- κB) site allowing induction during inflammatory reaction.[41] Immunostainings of GFAP,

UCH-L1, and MMP-9 are modified in HH alone or TBI+HH groups compared with TBI group but it seems to be more pronounced for MMP-9. Kolar et al[42] reported in 15 patients with severe TBI plasma kinetic of MMP-9 with increased levels on the first day and decreased levels on the third day, likely due to the restoration of BBB integrity. A second rise in MMP-9 levels was found on the fifth day, likely reflecting the development of secondary brain injury.

It is important to note that the changes found in GFAP, UCH-L1, and MMP-9 appear to be similar in the HH and TBI+HH groups. The modification observed could therefore better represent the effects of hypoxia-hypotension on the brain rather than the cumulative effects of TBI and HH.

Our study has some limitations. These findings represent only a static view of cerebral biomarker changes 4 hours after an experimental model of TBI in rat. It could be of interest to better characterize the temporal profile of these 3 biomarkers. Moreover, UCH-L1, GFAP, and MMP-9 have not been measured in plasma or CSF. Further studies are necessary to describe temporal profiles of these biomarkers in plasma and CSF after hypoxic insults and severe TBI.

We described here, after experimental TBI and hypoxia-hypotension in rats, global and regional changes for 3 biomarkers in the brain: GFAP, UCH-L1, and MMP-9. Immunostainings of UCH-L1 and MMP-9 increased in the TBI+HH group compared with the TBI group. Glial fibrillary acidic protein immunostaining decreased in the neocortex in the TBI+HH group compared with the TBI group. These three biomarkers could therefore be considered as potential biomarkers of hypoxia-hypotension insults independently of TBI.

Author Contributions

All authors had full access to all the data in the study and take responsibility for the integrity of the data and the accuracy of the data analysis. SM, LD, and TG contributed to conceptualization, methodology, investigation, and writing of original draft; FC and TA performed cerebral immunostaining; SM and LD performed formal analysis, collected resources, and contributed to visualization; SM, LD, FC, TA, JMC, OF, and TG contributed to writing, review, and editing; and TG contributed to supervision.

ORCID iD

Ségolène Mrozek ⓘD https://orcid.org/0000-0002-2370-6239

REFERENCES

1. Zitnay GA, Zitnay KM, Povlishock JT, et al. Traumatic brain injury research priorities: the Conemaugh International Brain Injury Symposium. *J Neurotrauma*. 2008;25:1135-1152. doi:10.1089/neu.2008.0599.
2. Tosetti P, Hicks RR, Theriault E, Phillips A, Koroshetz W, Draghia-Akli R. Toward an international initiative for traumatic brain injury research. *J Neurotrauma*. 2013;30:1211-1222. doi:10.1089/neu.2013.2896.
3. Berger RP, Houle J-F, Hayes RL, Wang KK, Mondello S, Bell MJ. Translating biomarkers research to clinical care: applications and issues for rehabilomics. *PM R*. 2011;3:S31-S38. doi:10.1016/j.pmrj.2011.03.016.
4. Chesnut RM, Marshall SB, Piek J, Blunt BA, Klauber MR, Marshall LF. Early and late systemic hypotension as a frequent and fundamental source of cerebral ischemia following severe brain injury in the Traumatic Coma Data Bank. *Acta Neurochir Suppl (Wien)*. 1993;59:121-125.
5. Mrozek S, Dumurgier J, Citerio G, Mebazaa A, Geeraerts T. Biomarkers and acute brain injuries: interest and limits. *Crit Care*. 2014;18:220. doi:10.1186/cc13841.
6. Papa L, Brophy GM, Welch RD, et al. Time course and diagnostic accuracy of glial and neuronal blood biomarkers GFAP and UCH-L1 in a large cohort of trauma patients with and without mild traumatic brain injury. *JAMA Neurol*. 2016;73:551-560. doi:10.1001/jamaneurol.2016.0039.
7. Huang X-J, Glushakova O, Mondello S, Van K, Hayes RL, Lyeth BG. Acute temporal profiles of serum levels of UCH-L1 and GFAP and relationships to neuronal and astroglial pathology following traumatic brain injury in rats. *J Neurotrauma*. 2015;32:1179-1189. doi:10.1089/neu.2015.3873.
8. Rosenberg GA, Yang Y. Vasogenic edema due to tight junction disruption by matrix metalloproteinases in cerebral ischemia. *Neurosurg Focus*. 2007;22:E4.
9. Zhang H, Adwanikar H, Werb Z, Noble-Haeusslein LJ. Matrix metalloproteinases and neurotrauma: evolving roles in injury and reparative processes. *Neuroscientist*. 2010;16:156-170. doi:10.1177/1073858409355830.
10. Mrozek S, Luzi A, Gonzalez L, Kerhuel L, Fourcade O, Geeraerts T. Cerebral and extracerebral vulnerability to hypoxic insults after diffuse traumatic brain injury in rats. *Brain Res*. 2016;1646:334-341. doi:10.1016/j.brainres.2016.06.007.
11. Blanié A, Vigué B, Benhamou D, Duranteau J, Geeraerts T. The frontal lobe and thalamus have different sensitivities to hypoxia-hypotension after traumatic brain injury: a microdialysis study in rats. *J Neurotrauma*. 2012;29:2782-2790. doi:10.1089/neu.2012.2381.
12. Geeraerts T, Friggeri A, Mazoit J-X, Benhamou D, Duranteau J, Vigué B. Posttraumatic brain vulnerability to hypoxia-hypotension: the importance of the delay between brain trauma and secondary insult. *Intensive Care Med*. 2008;34:551-560. doi:10.1007/s00134-007-0863-0.
13. Marmarou A, Foda MA, van den Brink W, Campbell J, Kita H, Demetriadou K. A new model of diffuse brain injury in rats. Part I: pathophysiology and biomechanics. *J Neurosurg*. 1994;80:291-300. doi:10.3171/jns.1994.80.2.0291.
14. Foda MA, Marmarou A. A new model of diffuse brain injury in rats. Part II: morphological characterization. *J Neurosurg*. 1994;80:301-313. doi:10.3171/jns.1994.80.2.0301.
15. Ract C, Vigué B, Bodjarian N, Mazoit JX, Samii K, Tadié M. Comparison of dopamine and norepinephrine after traumatic brain injury and hypoxic-hypotensive insult. *J Neurotrauma*. 2001;18:1247-1254. doi:10.1089/089771501317095287.
16. Holtzer S, Vigué B, Ract C, Samii K, Escourrou P. Hypoxia-hypotension decreases pressor responsiveness to exogenous catecholamines after severe traumatic brain injury in rats. *Crit Care Med*. 2001;29:1609-1614.
17. Paxinos G, Watson C. *The Rat Brain in Stereotaxic Coordinates*, 5th ed. Cambridge, MA: Academic Press; 2005.
18. Geng X, Zhang X, Zhou B, et al. Usnic acid induces cycle arrest, apoptosis, and autophagy in gastric cancer cells in vitro and in vivo. *Med Sci Monit*. 2018;24:556-566.
19. Kim M, Kim K-E, Jung HY, et al. Recombinant erythroid differentiation regulator 1 inhibits both inflammation and angiogenesis in a mouse model of rosacea. *Exp Dermatol*. 2015;24:680-685. doi:10.1111/exd.12745.
20. Abernathy LM, Fountain MD, Rothstein SE, et al. Soy isoflavones promote radioprotection of normal lung tissue by inhibition of radiation-induced activation of macrophages and neutrophils. *J Thorac Oncol*. 2015;10:1703-1712. doi:10.1097/JTO.0000000000000677.
21. Bishop P, Rocca D, Henley JM. Ubiquitin C-terminal hydrolase L1 (UCH-L1): structure, distribution and roles in brain function and dysfunction. *Biochem J*. 2016;473:2453-2462. doi:10.1042/BCJ20160082.
22. Mott JD, Werb Z. Regulation of matrix biology by matrix metalloproteinases. *Curr Opin Cell Biol*. 2004;16:558-564. doi:10.1016/j.ceb.2004.07.010.
23. Gu Z, Kaul M, Yan B, et al. S-nitrosylation of matrix metalloproteinases: signaling pathway to neuronal cell death. *Science*. 2002;297:1186-1190. doi:10.1126/science.1073634.
24. Li J, Yu C, Sun Y, Li Y. Serum ubiquitin C-terminal hydrolase L1 as a biomarker for traumatic brain injury: a systematic review and meta-analysis. *Am J Emerg Med*. 2015;33:1191-1196. doi:10.1016/j.ajem.2015.05.023.
25. Vos PE, Lamers KJB, Hendriks JCM, et al. Glial and neuronal proteins in serum predict outcome after severe traumatic brain injury. *Neurology*. 2004;62:1303-1310.
26. Grossetete M, Phelps J, Arko L, Yonas H, Rosenberg GA. Elevation of matrix metalloproteinases 3 and 9 in cerebrospinal fluid and blood in patients with severe traumatic brain injury. *Neurosurgery*. 2009;65:702-708. doi:10.1227/01.NEU.0000351768.11363.48.
27. Liu C-L, Chen C-C, Lee H-C, Cho D-Y. Matrix metalloproteinase-9 in the ventricular cerebrospinal fluid correlated with the prognosis of traumatic brain injury. *Turk Neurosurg*. 2014;24:363-368. doi:10.5137/1019-5149.JTN.8551-13.0.

28. Copin J-C, Rebetez MML, Turck N, et al. Matrix metalloproteinase 9 and cellular fibronectin plasma concentrations are predictors of the composite endpoint of length of stay and death in the intensive care unit after severe traumatic brain injury. *Scand J Trauma Resusc Emerg Med*. 2012;20:83. doi:10.1186/1757-7241-20-83.

29. Simon D, Evaldt J, Nabinger DD, et al. Plasma matrix metalloproteinase-9 levels predict intensive care unit mortality early after severe traumatic brain injury. *Brain Inj*. 2017;31:390-395. doi:10.1080/02699052.2016.1259501.

30. Zhao X, Ahram A, Berman RF, Muizelaar JP, Lyeth BG. Early loss of astrocytes after experimental traumatic brain injury. *Glia*. 2003;44:140-152. doi:10.1002/glia.10283.

31. Dunn-Meynell AA, Levin BE. Histological markers of neuronal, axonal and astrocytic changes after lateral rigid impact traumatic brain injury. *Brain Res*. 1997;761:25-41.

32. Ito J, Marmarou A, Barzó P, Fatouros P, Corwin F. Characterization of edema by diffusion-weighted imaging in experimental traumatic brain injury. *J Neurosurg*. 1996;84:97-103. doi:10.3171/jns.1996.84.1.0097.

33. Love KR, Catic A, Schlieker C, Ploegh HL. Mechanisms, biology and inhibitors of deubiquitinating enzymes. *Nat Chem Biol*. 2007;3:697-705. doi:10.1038/nchembio.2007.43.

34. Komander D, Clague MJ, Urbé S. Breaking the chains: structure and function of the deubiquitinases. *Nat Rev Mol Cell Biol*. 2009;10:550-563. doi:10.1038/nrm2731.

35. Majetschak M, King DR, Krehmeier U, et al. Ubiquitin immunoreactivity in cerebrospinal fluid after traumatic brain injury: clinical and experimental findings. *Crit Care Med*. 2005;33:1589-1594.

36. Caldeira MV, Salazar IL, Curcio M, Canzoniero LMT, Duarte CB. Role of the ubiquitin-proteasome system in brain ischemia: friend or foe? *Prog Neurobiol*. 2014;112:50-69. doi:10.1016/j.pneurobio.2013.10.003.

37. Hayashi T, Takada K, Matsuda M. Post-transient ischemia increase in ubiquitin conjugates in the early reperfusion. *Neuroreport*. 1992;3:519-520.

38. Lee S-R, Tsuji K, Lee S-R, Lo EH. Role of matrix metalloproteinases in delayed neuronal damage after transient global cerebral ischemia. *J Neurosci*. 2004;24:671-678. doi:10.1523/JNEUROSCI.4243-03.2004.

39. Vilalta A, Sahuquillo J, Rosell A, Poca MA, Riveiro M, Montaner J. Moderate and severe traumatic brain injury induce early overexpression of systemic and brain gelatinases. *Intensive Care Med*. 2008;34:1384-1392. doi:10.1007/s00134-008-1056-1.

40. Hadass O, Tomlinson BN, Gooyit M, et al. Selective inhibition of matrix metalloproteinase-9 attenuates secondary damage resulting from severe traumatic brain injury. *PLoS ONE*. 2013;8:e76904. doi:10.1371/journal.pone.0076904.

41. Rosenberg GA. Matrix metalloproteinases in brain injury. *J Neurotrauma*. 1995;12:833-842. doi:10.1089/neu.1995.12.833.

42. Kolar M, Pachl J, Tomasova H, Haninec P. Dymanics of matrix-metalloproteinase 9 after brain trauma—results of a pilot study. *Acta Neurochir Suppl*. 2008;102:373-376.